

Distance and extinction determination for APOGEE stars with Bayesian method

Jianling Wang^{1,2*}, Jianrong Shi^{1,2}, Kaike Pan³, Bingqiu Chen⁴, Yongheng Zhao^{1,2}, James Wicker²

¹ Key Laboratory of Optical Astronomy, NAOC, Chinese Academy of Sciences

² National Astronomical Observatories, Chinese Academy of Sciences, Beijing 100012, China

³ Apache Point Observatory and New Mexico State University, P.O. Box 59, Sunspot, NM, 88349-0059, USA

⁴ Department of Astronomy, Peking University, Beijing 100871.

Accepted ... Received ...

ABSTRACT

Using a Bayesian technology we derived distances and extinctions for over 100,000 red giant stars observed by the Apache Point Observatory Galactic Evolution Experiment (APOGEE) survey by taking into account spectroscopic constraints from the APOGEE stellar parameters and photometric constraints from 2MASS, as well as a prior knowledge on the Milky Way. Derived distances are compared with those from four other independent methods, the *Hipparcos* parallaxes, star clusters, APOGEE red clump stars, and asteroseismic distances from APOKASC (Rodrigues et al. 2014) and SAGA Catalogues (Casagrande et al. 2014). These comparisons covers four orders of magnitude in the distance scale from 0.02 kpc to 20 kpc. The results show that our distances agree very well with those from other methods: the mean relative difference between our Bayesian distances and those derived from other methods ranges from -4.2% to $+3.6\%$, and the dispersion ranges from 15% to 25%. The extinctions toward all stars are also derived and compared with those from several other independent methods: the Rayleigh–Jeans Color Excess (RJCE) method, Gonzalez’s two-dimensional extinction map, as well as three-dimensional extinction maps and models. The comparisons reveal that, overall, estimated extinctions agree very well, but RJCE tends to overestimate extinctions for cool stars and objects with low $\log g$.

Key words: stars: fundamental parameters – stars: distances – dust, extinction

1 INTRODUCTION

Galactic formation and evolution is one of the most outstanding problems in modern astrophysics. One way to address this question is through Galactic Archaeology, which is an approach to explore the formation and evolution history of the Milky Way through the “archeological” record provided by its individual stars. We are coming into a new era of Galactic investigation, in which Galactic archaeology can be studied with massive spectroscopic surveys. The spectra generated by these surveys are range from 10^4 to 10^7 , for examples, RAVE (Steinmetz et al. 2006), SEGUE (Yanny et al. 2009), APOGEE (Eisenstein et al. 2011; Majewski et al. 2010), GALAH (De Silva et al. 2015; Freeman 2012), LAMOST (Zhao et al. 2006; Cui et al. 2012), *Gaia* (Perryman et al. 2001; Lindegren 2010), ARGOS (Ness et al. 2012a,b), 4MOST (de Jong et al. 2012), and

WEAVE (Dalton et al. 2012). Valuable information, that can be extracted from these spectroscopic surveys, include fundamental stellar parameters, chemical compositions, and radial velocities of individual stars. With the compilations of these massive surveys in the next decade, our knowledge of Galactic formation and evolution will be significantly improved.

As a unique campaign among these surveys, APOGEE operates in the near-infrared band and is able to target stars at very low Galactic latitude (Zasowski et al. 2013), this penetrating the veil of interstellar dust. Besides observing disk stars, APOGEE also targets two other components: the halo and the bulge. It has pencil-beam observations of red giants in the halo that target fields in the bulge. The primary goal of APOGEE is to provide constraints on the dynamical and chemical evolution model of our Milky Way. Numerous Galactic structure and stellar population issues can be addressed by the APOGEE data. In order to take full advantage of this massive spectroscopic data set, and make a full use of the chemical information, we need to analyze the 6D phase-space dis-

* E-mail: wjianl@bao.ac.cn

tribution of stars in the Milky Way, which is usually hampered by a lack of reliable distance data.

The most accurate and successful direct distances measurements are from the *Hipparcos* satellite, which provide trigonometric parallaxes for $\sim 10^5$ stars. However, the *Hipparcos* measurements are only accurate to a distance around 200 pc (Burnett & Binney 2010). In the near future, the recently launched *Gaia* mission (Perryman 2005) will return parallax and proper motion measurements for around 10^9 stars, which will contribute to this field substantially. However, even after the *Gaia* mission is completed, stars with direct distance measurements are still less than 1% of all stars in the Milky Way. Indirect distance determination methods for more distant stars, especially for APOGEE stars with heavy extinction in the low latitude disk region, and in the bulge, are still highly desired.

Several indirect methods for determining stellar distance have been developed. Red Clump (RC) stars has been used as standard candles to calculate stellar distances (Bovy et al. 2014; Paczynski & Stanek 1998). Since the RC stage is very short in the whole stellar evolutionary life of a star, in general, this method is only suitable for a small fraction of stars. Asteroseismology can determine stellar parameters, such as stellar mass, radius, and age (Casagrande et al. 2014), with high precision. These parameters are then employed, together with other stellar parameters determined with classical methods, e.g., metallicity and effective temperature, to accurately estimate intrinsic stellar properties, such as distance and extinction. Rodrigues et al. (2014) have clearly demonstrated that distance can be obtained with high accuracy when coupled with asteroseismic information. However, the Asteroseismology method requires systematic variability studies of its targets. It not only needs the target stars to have detectable seismic activities, but also requires observing a very time consuming data set. Till now, only small patch of sky coverage has become available with Asteroseismology data (Koch et al. 2010), and many stars within the coverage area do have asteroseismic data for accurate distance determinations. Therefore, more general methods of deriving stellar distance are needed.

To take advantage of large sets of available spectroscopic and photometric data from recent surveys, more general methods to infer stellar parameters, such as extinction, mass, age, distance, etc, have been explored by many authors (Pont & Eyer 2004; Schönrich et al. 2014; Wang et al. 2016). Because of its importance, many among these works focus on distance determination (Breddels et al. 2014; Zwitter et al. 2010; Burnett & Binney 2010; Binney et al. 2014; Santiago et al. 2016; Wang et al. 2016). These authors use spectroscopic and photometric quantities to compute the probability distribution of stellar parameters, to infer distance of individual stars. The logistics of these works are similar, but different authors may implement the method in slightly different ways. For instance, some use estimated uncertainties of measured stellar parameters, some do not. Authors may treat extinction differently, use different theoretical evolutionary models, use different prior knowledge of the Galaxy, etc.

In this work, we follow the same Bayesian method as Wang et al. (2016) to derive distances for around 10^5 stars in the APOGEE survey. The extinction is considered consistently along with the distance determination. The plan for the paper is as follows. In Section 2, we briefly introduce the Bayesian method adopted in this work, while the APOGEE data from SDSS DR12 are described in Section 3. In Sections 4 and 5, we compare our Bayesian distances and extinctions with those from other independent methods. Finally, the conclusion is presented in Section 6.

2 BAYESIAN METHOD

The Bayesian method adopted here is the same as used by Wang et al. (2016), in which the distances and extinctions were calculated for around one million stars in the first data release of the LAMOST survey (Luo et al. 2015). The accuracy of the derived distances have been extensively tested with both simulation and several independent measurements utilizing LAMOST data. The check shows that a good accuracy can be achieved with the implemented Bayesian method in Wang et al. (2016). The method is very similar to those in Burnett & Binney (2010) and Binney et al. (2014). For clarity we give a brief description on this method.

For each star we have the relevant observables: effective temperature T_{eff} , metallicity [M/H], surface gravity $\log g$, and near infrared photometries J, H, K_s . These quantities form an observed vector:

$$\mathbf{O} = (T_{\text{eff}}, [\text{M}/\text{H}], \log g, J, H, K_s) \quad (1)$$

Each star can be related and characterized by a set of ‘‘intrinsic’’ parameters: metallicity [M/H], age τ , initial mass \mathcal{M} , position on the sky l, b , and distance from the Sun d . These quantities form another vector:

$$\mathbf{X} = ([\text{M}/\text{H}], \log \tau, \mathcal{M}, l, b, d) \quad (2)$$

With the help of trivial Bayesian theory, we can derive the posterior probability of $\mathbf{P}(\mathbf{X}|\mathbf{O})$, which is the conditional probability of the parameter set \mathbf{X} given \mathbf{O} .

$$P(\mathbf{X}|\mathbf{O}) = \frac{P(\mathbf{X})}{P(\mathbf{O})}P(\mathbf{O}|\mathbf{X}), \quad (3)$$

\mathbf{O} and \mathbf{X} can be connected by theoretical isochrones, with \mathbf{O} being a function of \mathbf{X} . $\mathbf{P}(\mathbf{O})$ is the probability that the set of observations was made and does not depend on \mathbf{X} , which is a normalization factor. $\mathbf{P}(\mathbf{O}|\mathbf{X})$ is the probability that the set of observations \mathbf{O} gives the set of parameters \mathbf{X} . We assume the uncertainties of the measured observables for each component of \mathbf{O} can be described as a Gaussian distribution with a mean $\tilde{\mathbf{O}}$ and standard deviation $\sigma_{\tilde{\mathbf{O}}}$.

$$P(\tilde{\mathbf{O}}|\mathbf{X}) = G(\tilde{\mathbf{O}}|\mathbf{O}(\mathbf{X}), \sigma_{\mathbf{O}}) = \prod_{(i=1)}^n G(\tilde{O}_i|\mathbf{O}(\mathbf{X}), \sigma_{oi}) \quad (4)$$

$\mathbf{P}(\mathbf{X})$ is the prior probability we ascribe to the set of parameters, which is an important ingredient in the Bayesian method. Burnett & Binney (2010) used a three-component prior model of the Galaxy for the distribution functions of metallicity, density, and age:

$$P(\mathbf{X}) = p(\mathcal{M}) \sum_{i=1}^3 p_i([\text{M}/\text{H}]) p_i(\tau) p_i(\mathbf{r}) A_{V_{\text{prior}}}(\ell, b, d) \quad (5)$$

Where the $i = 1, 2, 3$ correspond to thin-, thick-disk, and stellar halo, respectively. A slightly modified Kroupa-type IMF is adopted as shown in Burnett & Binney (2010) and Binney et al. (2014). The same as Binney et al. (2014), an extinction prior, which employs the three-dimensional Milky Way extinction model, is used to calculate the extinction by integrating along each line of sight toward individual stars.

Having the posterior probability distribution function, $P(\mathbf{X}|\tilde{\mathbf{O}})$, the mean and standard deviation for each parameters in \mathbf{X} can be obtained by taking the first and second moments of this distribution as shown by Burnett et al. (2011). Besides providing the distance (d), this Bayesian method can also output an-

other distance estimator, the parallax ($\langle\varpi\rangle$). In general, there is the relation between these two distance estimators, $\langle d \rangle \gtrsim 1/\langle\varpi\rangle$, which can be attributed to the weights that each estimator attaches to the possibilities of long or short distance (Binney et al. 2014). Binney et al. (2014) find that $1/\langle\varpi\rangle$ is a good distance estimator for RAVE data. In this work, we will use the output $\langle d \rangle$ directly in the following sections. However, for comparison we also list the results estimated from $\langle\varpi\rangle$ in Table.1.

The Padova isochrones¹ (Marigo et al. 2008; Marigo & Girardi 2007; Girardi et al. 2000; Bertelli et al. 1994) are adopted like in Wang et al. (2016). The metallicity steps of the isochrones have been carefully chosen by Burnett & Binney (2010) for avoiding great changes in the observed quantities between adjacent isochrones, and have been extended to low metallicity by Wang et al. (2016).

Since the extinction can be calculated with this Bayesian method, an extinction law is a necessary ingredient. At present, there is no real consensus on the correct extinction law along all the directions of the Galaxy, especially toward to the Galactic bulge region (Gonzalez et al. 2012; Nishiyama et al. 2006, 2008, 2009). Thus, we decide to use the extinction law of Cardelli et al. (1989, CCM) with $R_V = 3.1$ as shown in Wang et al. (2016).

3 DATA SAMPLES

The Apache Point Observatory Galactic Evolution Experiment (APOGEE) as one component of SDSS III (Eisenstein et al. 2011), is a near-infrared (H -band; $1.51\mu\text{m} \sim 1.70\mu\text{m}$), high-resolution ($R \sim 22,500$) spectroscopic survey. It targets primarily red giant (RG) stars across all Galactic environments and stellar populations in the Milky Way (Allende Prieto et al. 2008; Majewski et al. 2010), using the Sloan 2.5 m telescope (Gunn et al. 2006) and an innovative multi-object IR spectrograph (Wilson et al. 2010). The stellar atmospheric parameters and individual chemical abundances are derived from combined APOGEE spectra with the APOGEE Stellar Parameters and Chemical Abundances Pipeline (ASPCAP; García Pérez et al. 2015), which finds the best matching between pre-calculated synthetic spectra to the observed ones via a χ^2 minimization. To validate ASPCAP outputs, stellar parameters for members in well studied clusters and surface gravities from asteroseismic analyses are carefully compared (Mészáros et al. 2013). Calibration correlations are applied to the original ASPCAP outputs to obtain calibrated stellar parameters for stars (Holtzman et al. 2015). The empirical uncertainty of T_{eff} is about 100 K through comparison of ASPCAP derived temperatures with photometric temperatures, and 0.11 dex for $\log g$ via comparing calibrated ASPCAP values with asteroseismic surface gravities for stars in the *Kepler* field. The internal precision of the APOGEE abundances is typically 0.05 – 0.1 dex, but the external accuracy of the abundances is challenging to assess, and may only be good to 0.1-0.2 dex (Holtzman et al. 2015). It is worthy to note that the applied calibration correlations are derived with members in well-studied clusters and stars in the *Kepler* field; their reliability outside parameter spaces that these calibrated stars cover, such as surface gravities of metal poor stars, are not validated.

The final SDSS-III APOGEE public data release, DR12 (Alam et al. 2015), includes catalogs with radial velocity, stellar parameters (T_{eff} , $\log g$, $[M/H]$, $[\alpha/M]$), and 15 elemental abundances

for over 150,000 stars, as well as more than 500,000 spectra from which these quantities are derived. We retrieved the calibrated stellar parameter data from the APOGEE Parameter Catalogs of SDSS DR12 using the CasJobs interface². The Two Micron All Sky Survey (2MASS) near-infrared photometric data for the same stars in $J(1.24\mu\text{m})$, $H(1.66\mu\text{m})$, $K_s(2.16\mu\text{m})$ are also extracted from the point-source catalogue (Cutri et al. 2003; Skrutskie et al. 2006). The following procedure is used to select stars with reliable parameters: First, stars should not be set any flags indicating that the observations or analysis is bad. Second, stars without any calibrated parameters (such as dwarfs) are excluded. We use SDSS CasJobs to extract the data with the following command scripts: (aspcapflag & dbo.fApogeeAspcapFlag('STAR.BAD')) = 0 and Teff > 0. With these criteria, we select 104816 stars from the APOGEE catalogue. There are 3084 stars that have been observed more than once. For stars with multiple observations, only data with the highest signal to noise ratio are used. This results in 101726 stars in our final sample. We note that in the following analysis only stars with $T_{\text{eff}} < 5200$ K and $\log g < 3.8$ are used to select stars with reliable parameters (Holtzman et al. 2015), and there are 99165 stars left after applying this selection. After further strict criteria are applied, such as $T_{\text{eff}} > 3800$ K and ASPCAP_CHI2 < 20 (92060 stars left), no significant change is noticed in the statistical results.

4 EXTERNAL COMPARISONS ON DERIVED DISTANCES

As discussed above, there are several independent methods which can deliver reliable distances for their suitable targets. For instance, distances to nearby stars from parallax measurements; to cluster members from the main-sequence fitting, distances of red clump (RC) stars by using them as a distance candle; distances of giants from asteroseismic information, etc. Our Bayesian method, described in Section 2, is a more general one. In principle, it can be used to derive stellar distances of individual stars which have available spectroscopic and photometric quantities. To validate our derived stellar distances, we compare our derived distances with results from other independent methods for common stars: astrometric parallax distances obtained by ESA's *Hipparcos* mission (van Leeuwen 2007); distances to well studied clusters, distances of RC stars, and distances from asteroseismic analyses. Figures 1 to 6 show these comparisons which are also summarized in Table 1. In summary, the systematic offsets, in terms of our derived distances minus others', range from -4.2% to 3.6% , with dispersions from 15% to 25%; considering mutual uncertainties in our derived distances and in others', our distances are consistent with those from other methods. We discuss these comparisons in more detail below.

4.1 Samples with Accurate *Hipparcos* Distances

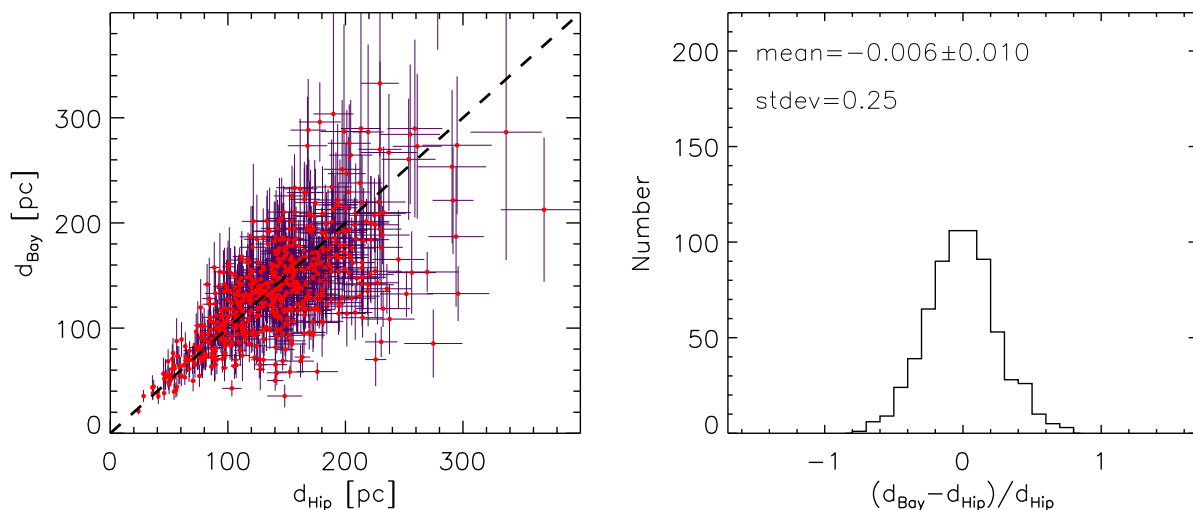
The *Hipparcos* mission measured trigonometric parallaxes of $\sim 10^5$ nearby stars. van Leeuwen (2007) improved the measured distances of the *Hipparcos* stars through a re-reduction process. It is believed that the van Leeuwen (2007) catalogue contains the most accurate set of distance measurements for nearby stars ($d < 300$ pc). Therefore, here we compare our derived distances with those from the van Leeuwen (2007) catalogue for common stars between APOGEE data set and *Hipparcos* stars.

¹ <http://stev.oapd.inaf.it/cgi-bin/cmd>

² <http://skyserver.sdss.org/casjobs/>

Table 1. Summary the relative difference between our Bayesian distances and reference distance samples. Two distance estimators from Bayesian methods are used for comparison.

Samples	N _{stars}	Dist. Range (kpc)	distance is derived from $1/\langle\varpi\rangle$		$\langle d \rangle$ is used for distance	
			Relative residual(%)		Relative residual(%)	
			Mean	R.M.S.	Mean	R.M.S.
Hipparcos	662	0.02-0.2	-3.8 ± 1.0	25	-0.6 ± 1.0	25
APOGEE-clusters	431	0.8-19.3	-5.5 ± 1.0	20	-4.2 ± 1.1	18
APOGEE-RC	19937	0.4-12.5	-3.3 ± 0.1	17	-1.2 ± 0.1	18
Rodrigues et al.	1989	0.3-4.7	$+1.2 \pm 0.3$	15	$+3.6 \pm 0.3$	16
SAGA	135	0.7-4.1	-2.1 ± 0.7	15	$+0.0 \pm 0.8$	15

**Figure 1.** Left panel: comparison of distances to stars derived from our Bayesian method (d_{Boy}) with those from the *Hipparcos* parallaxes (d_{Hip}) with $\sigma_{\varpi}/\varpi < 0.1$. The horizontal error bars are derived from uncertainties of the *Hipparcos* parallaxes, while the vertical error bars are from the formal error outputted by the Bayesian method explained in Section 2. Right panel: fractional difference distribution of distances with mean value and dispersion labeled on the top. The error of the mean value in the right panel is estimated by the bootstrap method with 1000 samples.

An ancillary APOGEE project, observing bright nearby stars which have *Hipparcos* parallax measurements, is setup. It would be a very inefficient way to use available resources if the regular APOGEE survey mode, the Sloan 2.5m telescope + APOGEE spectrograph, is used to observe these bright objects because there are not enough bright objects for all 300 fibers in a field and this requires a high observational overhead due to short exposure time. Therefore, 10 fibers were installed to connect the APOGEE instrument to the NMSU (New Mexico State University) 1m telescope. This configuration allows one science fiber and nine sky fiber per observation. Bright stars with magnitudes of $0 < H < 8$ are observed in this configuration. The NMSU 1m+APOGEE is used during dark time when the APOGEE instrument is not used with the Sloan 2.5m Telescope (see Feuillet et al, 2015 for more details).

The spectra taken with the NMSU 1m+APOGEE are reduced and analyzed with the ASPCAP pipeline (Holtzman et al. 2015). Compared to the main survey data, a different method was needed to treat the telluric absorption because no hot, relatively featureless star could be observed simultaneously. The atmospheric model spectrum is combined with a spectral template that best fits the target and is adjusted to fit the telluric features in the observed target spectrum. This process is iterated to produce the telluric absorption spectrum that best matches the observed spectrum (Feuillet et al. 2016). Similar to the main survey, sky emission features are sub-

tracted with data from sky fibers. Because there are more sky fibers which can also be placed closer to the target star, in the NMSU 1m+APOGEE observations, presumably, sky emission features can be removed better. The stellar parameters and abundances are then derived from the spectra with ASPCAP (García Pérez et al. 2015). Overall, stellar parameters and abundances for stars that are observed with the NMSU 1m+APOGEE are obtained in an almost identical way as for the APOGEE main survey.

Hundreds of stars with parallax error $< 10\%$ were selected from the *Hipparcos* Catalog van Leeuwen (2007). 750 of them were observed with the NMSU 1m+APOGEE and included in SDSS DR12. However, 45 of them that are outside the ASPCAP calibration range ($\log g > 3.8$, $(J - K) > 0.5$) are excluded from Feuillet et al. (2016)'s analysis. We thank Feuillet for sharing this target list. For these 705 stars, the mean difference between our derived distances and the *Hipparcos* distances is $1.4 \pm 1.0\%$, with an rms of 25%. Compared to distances from Santiago et al. (2016), our derived distances agree with *Hipparcos* distances slightly better, but are comparable. (For the same data set, they have distance difference residual and rms of 1.6% and 26.4%, respectively.) Feuillet et al. (2016) applied a slightly different cut than ours to get the list of 705 stars. In the list, there are still some stars whose T_{eff} are above the cut limits we applied, i.e. $T_{\text{eff}} < 5200K$. To be consistent with other comparison, we excluded these stars from

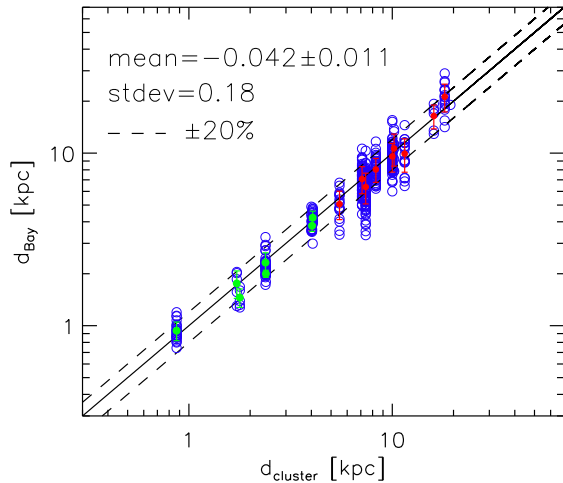


Figure 2. Estimated distances to cluster stars plotted against the cluster distances from the literature, and star members of clusters are identified by Mészáros et al. (2013). The solid line indicates identity, while the dashed-line shows the distances that differ by 20%. The mean relative difference and dispersion are labeled at the top right of the figure. The blue open circles are for individual stars, while the red and green solid circles indicate the mean distances derived from stars belonging to global clusters and open clusters, respectively, and the error bars indicate the dispersion for each of the clusters.

the list. To exclude stars in possible multiple systems, we also limit our objects to likely single stars, i.e. those with $\text{Soln} > 10$ in the van Leeuwen (2007) catalogue. This process leads to 662 reminding. For these 662 stars, the mean difference between our derived distances and those from *Hipparcos* is $-0.6 \pm 1\%$, with an rms of 25%. This comparison is shown in Fig. 1.

4.2 Members of Well-Studied Clusters

559 stars in 20 star clusters are used for the APOGEE calibration (Mészáros et al. 2013). The identifications of these cluster members are listed in their Table 4. These members provide a good opportunity to check the reliability of our derived distances via comparing our distances with those from a cluster with independent methods.

Among 559 stars used by Mészáros et al. (2013), all are members of two open clusters M35 and Pleiades, but are not included in the new data release SDSS DR12. For better quality of APOGEE stellar parameters, we also excluded targets with $T_{\text{eff}} > 5200$ K and $\log g > 3.8$ (see Holtzman et al. 2015). This leaves us with 437 stars from 11 global clusters and 7 open clusters, of which 332 stars are in global clusters and 105 are in open clusters. Distances of the 18 clusters are searched from literature, and listed in Table 2 below. Only recent measurements, later than 2009, are used. Otherwise, distances in Open Cluster Catalogues (Dias et al. 2002) and in the Global Cluster Catalogue (Harris 1996, 2010 edition) are used.

Distances of these 437 stars are derived with the Bayesian method as described in Section 2. As always, identifying cluster members is not trivial work. It is very possible that a few stars in Table 4 of Mészáros et al. (2013) are not true cluster members since their targets include stars with a probability $> 50\%$ of being a cluster member based on their proper motions. Furthermore, it is possible that cluster members interact each other due to the crowdedness of the field; such interactions might result in blue stragglers or

other outcomes. Clusters also have a high fraction of binary or multiple systems. The evolution status of cluster members will change if they experience interactions between (among) cluster members, and become components of binary or multiple systems. So, their observational vector, $O = (T_{\text{eff}}, [M/H], \log g, J, H, K_s)$, will deviate from their intrinsic ones. As a result, our derived distances of these members, which are based on their observational vectors, will deviate from the true cluster distance. This results in outliers in our derived distances to cluster members. To exclude these outliers and possible “false” cluster members in the target selection, we discarded six stars whose derived distances are less than one half of the mean distances of other members in the same cluster, or are greater than 1.8 times the mean distance.

Fig. 2 shows a comparison between our derived distances of individual star versus cluster distances listed in Table 2. The cluster distances range from ~ 0.8 kpc to ~ 20 kpc. For the whole sample, the mean difference is -4.2 ± 1.0 percent, in terms of our derived distances minus corresponding cluster distances, with a dispersion of 18 percent. Individually, most clusters have mean differences of $< 10\%$ with scatters of less than 18%, except for NGC 7789, M5, and M53 which have mean difference residuals of -18% , -14% , and $+13\%$, respectively. In groups of open and global clusters, they have mean differences of $(-0.9 \pm 1.7)\%$ and $(-5.2 \pm 1.9)\%$, and dispersions of 13% and 19%. The group of open clusters has a better comparison than the global clusters in both the mean difference and the dispersion. The result is not unexpected for two reasons. First, our derived distances toward individual cluster members depend on quality of observational quantities in the observed vector, i.e. T_{eff} , $[M/H]$, $\log g$, J , H , and K_s (see Section 2). In SDSS DR12, offsets have been applied to stellar parameters from ASPCAP (García Pérez et al. 2015) based on calibrations with clusters, standard stars, and stars in the *Kepler* field. Among these observational quantities, $\log g$ is the most important one for deriving distances to individual stars, because surface gravities in SDSS DR 12 are calibrated via asteroseismic analysis in the *Kepler* field and stars in the field have similar metallicities as those of open cluster members. By contrast, global clusters have much lower $[M/H]$. Therefore, we expect that stellar parameters of our open cluster members are better calibrated than those of global cluster ones. In other words, we expect that our derived distances to open cluster members are more reliable than those to global cluster stars. Secondly, globular clusters are much more crowded than open clusters, and they are usually much farther. So, listed distances of open clusters in Table 2 are usually more accurate than those of globular clusters.

Santiago et al. (2016) also derived distances for the same set of cluster members. Their derived distances are 16.5% greater than cluster distances with an rms of 29.9%. In both the mean difference and dispersion, our distances appear to agree with cluster distances better than theirs. However, we use cluster distances from the most recent measurements when they are available whereas Santiago et al. (2016) adopted cluster distances from cluster catalogues (Dias et al. 2002; Harris 1996, 2010 edition). Our adopted new distance measurements may explain part of our better comparison.

Cluster distances, including those listed in Table 2, are usually derived by main sequence fitting, white dwarf fitting, period-luminosity relation, proper motions, etc. Most methods are somewhat model dependent. As Santiago et al. (2016) argued, isochrone-based cluster distances are subject to a zero-point shift. Each method suffers its own uncertainties. It is not unusual that distances of the same cluster determined with different methods or

Table 2. Cluster Distances from Literature.

Cluster ID	Name	Distance (kpc)	Reference
NGC 4147		19.3	Harris (1996, 2010 edition)
NGC 5024	M53	18.1 ± 0.4	Dékány & Kovács (2009)
NGC 5272	M3	10.0 ± 0.2	Dalessandro et al. (2013)
NGC 5466		16.0	Harris (1996, 2010 edition)
NGC 5904	M5	7.4 ± 0.1	Coppola et al. (2011)
NGC 6171	M107	5.5	O’connell et al. (2011)
NGC 6205	M13	7.1 ± 0.14	Dalessandro et al. (2013)
NGC 6341	M92	8.3 ± 0.2	Harris (1996, 2010 edition)
NGC 6838	M71	4.0	Harris (1996, 2010 edition)
NGC 7078	M15	10.2 ± 0.2	Harris (1996, 2010 edition)
NGC 7089	M2	11.5	Harris (1996, 2010 edition)
NGC 188		1.72 ± 0.07	Wang et al. (2015); Jacobson et al. (2011)
NGC 2158		4.03 ± 0.13	Jacobson et al. (2011)
NGC 2420		2.39 ± 0.29	Jacobson et al. (2011)
NGC 2682	M67	0.87 ± 0.15	Sarejedini et al. (2009); Jacobson et al. (2011)
NGC 6791		4.06 ± 0.15	An et al. (2015)
NGC 6819		2.38 ± 0.10	Wu et al. (2014)
NGC 7789		1.78 ± 0.06	Wu et al. (2009)

by different individuals differ by 10%. Therefore, taking into account mutual uncertainties in both distances, those listed in Table 2 and in our new derived distances, we conclude that these new derived Bayesian distances agree very well with cluster distances from different methods. Based on the fact that our over 100 open cluster members have a mean difference of $(-0.9 \pm 1.7)\%$, and a dispersion of 13%, we believe that the Bayesian Method can deliver reliable stellar distances assuming their stellar parameters are well determined.

4.3 Red clump stars in the APOGEE-RC catalogue

The red clump star corresponds to the core-helium-burning stage in the stellar evolution of low-mass stars, and the luminosity distribution of this type of star is very narrow, e.g. their absolute magnitude at peak does not depend strongly on the age and metallicity (Groenewegen 2008), thus, they have frequently been used as distance standard candles (Williams et al. 2013).

Recently, Bovy et al. (2014) developed a new method for selecting individual likely red clump stars from spectrophotometric data by combining cut in $(\log g, T_{\text{eff}}, [\text{Fe}/\text{H}], [J - K_s]_0)$ and calibrating with high quality seismic $\log g$ data from a sub-sample of the APOGEE stars with measured oscillation frequencies from the *Kepler* (Gilliland et al. 2010) mission. This method results in a sample with high purity, and it is estimated that the contamination is less than 3.5 percent (Bovy et al. 2014). The newly released APOGEE-RC catalogue in SDSS DR12 contains 19,937 stars, which is around 20 percent of the whole APOGEE sample. In other words, distances towards 80% of stars in the APOGEE survey cannot be obtained via the RC distance candle.

Bovy et al. (2014) derived distances toward their identified RC stars, and estimated that the distance uncertainty is 5%–10%. In Fig. 3, we plot our derived distances versus those from Bovy et al. (2014). The left panel presents the one-to-one correspondence, while the right panel shows the relative difference distribution. The mean relative difference in terms of $(d_{\text{ours}} - d_{\text{RC}})/d_{\text{RC}}$ is -1.2 ± 0.1 percent with an rms of 18%. It should be noted that this comparison uses all stars in the APOGEE-RC catalogue which includes some misclassified RGB stars (Bovy et al. 2014). RC-

distances from Bovy et al. (2014) towards these misidentified RC stars will be off of their true values.

4.4 Stars with asteroseismic Distance

Recently, Rodrigues et al. (2014) derived the distances and extinctions for 1989 stars in the APOKASC Catalogue (Pinsonneault et al. 2014) with a Bayesian method. The method took into account the spectroscopic constraints derived from APOKASC and the asteroseismic parameters from the *Kepler* asteroseismic Science Consortium (KASC). They used the code PARAM³ (da Silva et al. 2006) to estimate the stellar properties by comparing observation data with those derived from a stellar model via a Bayesian method. In their work, two steps have been used to derive the distance and extinction. Firstly, from the observables $(T_{\text{eff}}, [\text{M}/\text{H}], \Delta\nu, \nu_{\text{max}})$, they used PARAM to derive a probability density function (PDF) for a set of parameters: $\mathcal{M}, R, \log g$, $\text{age}(\tau)$, and absolute magnitudes of several passbands M_λ . In the second step, they used T_{eff} and $[\text{M}/\text{H}]$ derived from spectroscopic observation, as well as the asteroseismic $\log g$ to derive the PDF of the absolute magnitudes for given passbands. With PDF for each passband, the joint PDF of the distance modulus can be obtained after accounting for the extinction. Distances and extinctions of 1989 stars were obtained with constraints from asteroseismic $\log g$, spectroscopic constraints of T_{eff} and $[\text{M}/\text{H}]$ from SDSS DR10 (Ahn et al. 2014), and photometry constraints from SDSS, 2MASS, and WISE data. Because of the highly accurate $\log g$ values that are well constrained by their available asteroseismic information, the distances can be determined with high precision (Rodrigues et al. 2014). The internal uncertainties of the derived distance are a few percent (Rodrigues et al. 2014). Such highly accurate distance data are desirable for the study of Galactic Archaeology. However, the majority of APOGEE stars do not have asteroseismic information, so their distances cannot be derived via this method, i.e. with asteroseismic constraints. Comparing these accurate distances with those from our Bayesian method,

³ <http://stev.oapd.inaf.it/param>

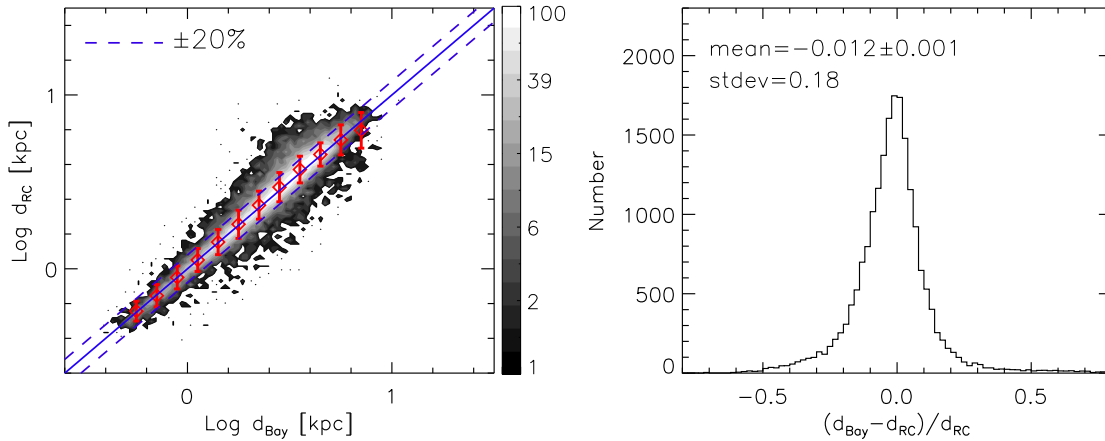


Figure 3. Left panel: Comparing distances derived by our Bayesian method (d_{Bay}) to that from Bovy et al. (2014) for red clump stars (d_{RC}). The blue solid line shows the identity, and two dashed lines indicate distances differ by 20% for guidance. Right panel: the histogram of the distribution of relative difference with mean value and dispersion being labeled on the top. The error of mean value is estimated by the bootstrap method with 1000 samples.

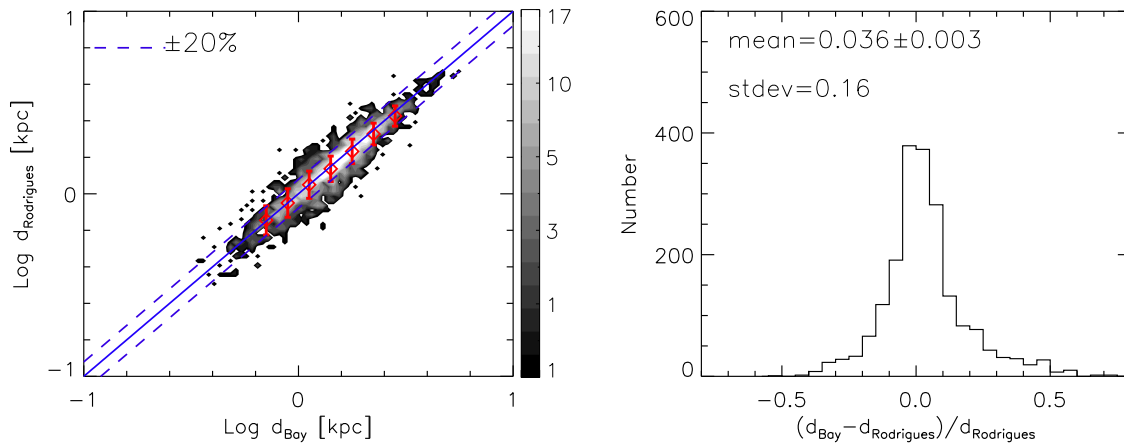


Figure 4. Left panel: Comparison of distances derived from our Bayesian method (d_{Bay}) with those from Rodrigues et al. (2014) ($d_{\text{Rodrigues}}$) for stars with asteroseismic information available in the *Kepler* field. The blue solid line and dashed-lines show the identity and distances that differ by 20% for guidance. The red diamonds and error bars are the mean value and dispersion in each bin respectively. Right panel: the histogram of the relative difference distribution with mean value and dispersion being labeled on the top. The error of mean difference is estimated by the bootstrap method with 1000 samples.

which does not require asteroseismic information, will be useful to quantify the accuracy of our determination.

The results are shown in Fig.4. The left panel presents a one-to-one correspondence, while the right panel indicates the distribution of the fractional difference. The mean fractional difference is 3.6 ± 0.3 per cent with a scatter of 16 per cent. Although both Rodrigues et al. (2014) and we use Bayesian methods, the two studies use different approaches (see Section 2 and the previous paragraph): different prior functions are adopted, Rodrigues et al. (2014) used T_{eff} and $[M/H]$ from SDSS DR10 whereas ours are from SDSS DR12, Rodrigues et al. (2014) used photometry information from more bandpasses than we do. The difference may also arise from the surface gravity used in Rodrigues et al. (2014) and ours, to which the distances are much sensitive. Rodrigues et al. (2014) used asteroseismic information directly, while we adopted the $\log g$ from the calibrated parameters of ASPCAP. The nominal uncertainty of calibrated $\log g$ from ASPCAP is 0.11 dex, however, the true error is likely to be dominated by systematics (Holtzman et al. 2015). It is possible that the mean difference and the scatter are due to the combination of the differences in the

two methods. It is worth noting that the median difference is only 1.7 ± 0.3 per cent in this comparison. Meanwhile, if our other distance indicator, $1/\langle\varpi\rangle$, is used, both the mean difference and the scatter will be smaller, 1.2% and 15%.

Casagrande et al. (2014) released the first results from the ongoing Strömgren survey for Asteroseismology and Galactic Archaeology (SAGA) in the *Kepler* field. They derived the stellar parameters by coupling of classic and asteroseismic parameters iteratively and self-consistently: e.g. effective temperatures from IRFM, metallicities from Strömgren indices, and masses and radii from seismology. This data set is limited by the *Kepler* and Strömgren surveys, so only a small strip of sky coverage centered at a Galactic longitude of 74° and covering latitude from about 8° to 20° is available. Their first release only includes ~ 1000 stars, but the typical precision of their derived distances is high, at a few percent (Casagrande et al. 2014). We cross-matched Casagrande et al. (2014)’s catalogue with the APOGEE stars, and found 135 matches. We compare our derived distances with those from the catalogue. The results are presented in Fig.5. Surprisingly,

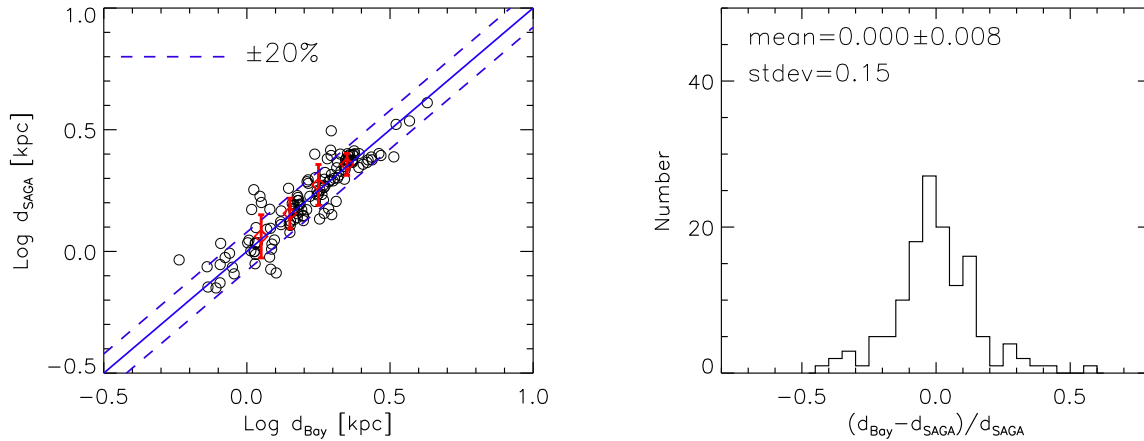


Figure 5. Left panel: Comparing distances from this work (d_{Bay}) with those from Casagrande et al. (2014) (d_{SAGA}) for the SAGA catalogue. The black open circles show individual stars, while the red solid circles and error bars indicate the mean values and the dispersion. The blue solid line denotes the identity and dashed-lines show differences at $\pm 20\%$ for guiding eyes. Right panel: the histogram of the relative difference with mean value and dispersion being labeled on the top. The error of the mean value is estimated by the bootstrap method with 1000 samples.

There is nearly no systematical offset, and the dispersion is 15 per cent.

No systematic offset between the two sets of derived distances is a somewhat surprising result because there are differences in the underlying methods, in isochrones used, and spectroscopic stellar parameters used. Casagrande et al. (2014) derived the stellar parameters in a different way than the APOGEE pipeline, and there are systematic differences in the derived parameters from these two different methods, i.e. their T_{eff} s are about 90 K hotter than those from ASPCAP, and $[M/H]$ s are ~ 0.14 dex lower. The differences in T_{eff} and $[M/H]$ could introduce a $\sim 2\%$ systematic difference in derived distances (Rodrigues et al. 2014). It is possible that the difference introduced by T_{eff} and $[M/H]$ is offset by ones due to other differences, such as methods and isochrones.

5 EXTINCTION

5.1 Comparison with extinction from Rodrigues et al. (2014)

Rodrigues et al. (2014) obtained distances and extinctions of stars with the asteroseismic constraints. It is believed that these extinctions are very accurate, thus, it is instructive to compare our extinctions with theirs. Fig.6 compares our results with those of Rodrigues et al. (2014). The left panel presents a one-to-one correspondence for each star, while the histogram of the extinction difference in the K_s -band is shown in the right panel. The plots show that the two sets of extinctions agree very well. The mean difference is only 0.01 Mag.. It is worth noting that, unlike Rodrigues et al. (2014), our Bayesian method does not return any (nonphysical) negative $A(K_s)$.

The *Kepler* field is a low extinction region, so the extinctions towards most stars are less than 0.07 Mag. in K_s -band, which corresponds to 0.6 Mag. in A_V . This value is much lower than that in the disk region, where most APOGEE targets are located. Thus, in the following section we compare our extinction with those from other methods.

5.2 Comparison with Extinctions from RJCE and from the Two-dimensional Extinction Map

To derive the extinction corrections, the Rayleigh Jeans Color Excess (RJCE) method has been adopted in the APOGEE targeting (Majewski et al. 2011). RJCE calculates reddening values on a star-by-star basis using a combination of near- and mid-IR photometry. This method assumes that all stars have a specific color in $(H - [4.5\mu\text{m}])_0$.

$$A(K_s) = 0.918(H - [4.5\mu\text{m}] - (H - [4.5\mu\text{m}])_0), \quad (6)$$

The $4.5\mu\text{m}$ photometric data are either from *Spitzer*-IRAC data (Werner et al. 2004; Fazio et al. 2004) or *WISE* surveys (Cutri et al. 2013). Majewski et al. (2011) estimated an approximate RJCE extinction uncertainty of $\lesssim 0.11$ Mag. for a typical star. The RJCE method has been widely used for individual stellar extinction corrections in APOGEE target selection. We extracted extinction values for stars with the *ak_targ_method* flag set to “RJCE” in SDSS DR 12, and compare with our derived extinctions for the same stars.

We also compared our extinctions with those from the two-dimensional extinction map of Gonzalez et al. (2012, G12), which was constructed based on measuring the mean $J - K_s$ color of the red clump stars in the bulge area. This extinction map has a resolution limit of $2'$. Using the BEAM calculator Web page⁴, we retrieved the extinction for each star in the map with the criterion of being the closest with $2'$ of its position.

Fig.7 shows the extinction difference between ours and those from RJCE (left column), and those from Gonzalez et al. (2012) as functions of the stellar atmospheric parameters, T_{eff} , $\log g$, $[M/H]$. In general, the extinction derived from RJCE and Gonzalez et al. (2012) agree well with ours, with a discrepancy of $A(K_s) \lesssim 0.2$ Mag. However, we note that, for cool giants, the extinction from RJCE is systematically higher than ours; this trend, as also seen in Wang et al. (2016), can be explained by the dependence of the RJCE method on the spectral type, which is clearly shown in Fig.1 of Majewski et al. (2011). At low temperature the intrinsic color of $(H - [4.5\mu\text{m}])_0$ increases with decreasing temperature,

⁴ <http://mill.astro.puc.cl/BEAM/calculator.php>

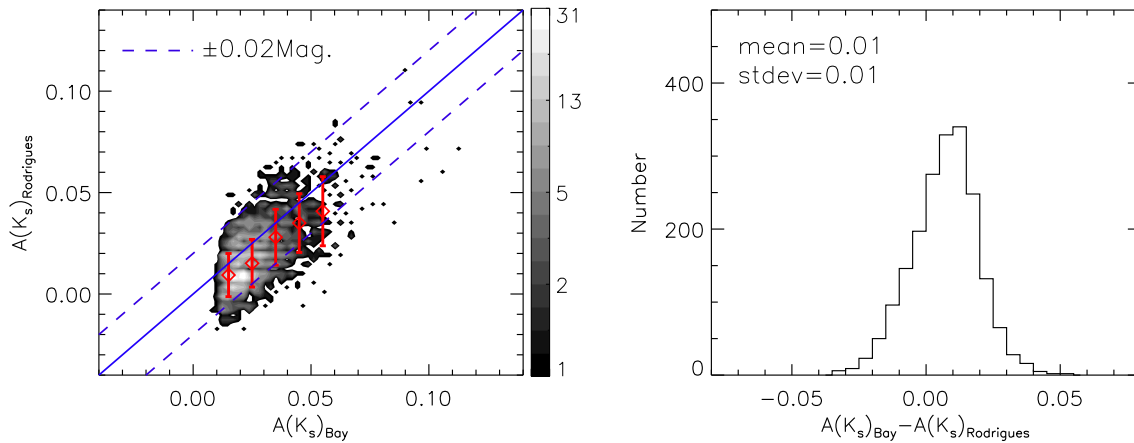


Figure 6. Left panel: compares extinction in K_s band derived from our Bayesian method, $A(K_s)_{\text{Bay}}$, with that derived by Rodrigues et al. (2014), $A(K_s)_{\text{Rodrigues}}$, for stars in the *Kepler* fields. The solid blue line shows the identity, while the dashed blue lines indicate the extinction differs by 0.02 Mag. The red symbols show the mean value, while the error bars indicate the dispersion. Right panel: the histogram of extinction difference with mean and dispersion being labeled on the top.

which results in overestimating the extinction, $A(K_s)_{\text{RJCE}}$. In the metallicity panel, $A(K_s)_{\text{RJCE}}$ seems overestimated for stars with $[M/H] < -1$. These trends are not manifested in the comparison between our extinctions and those from Gonzalez et al. (2012). Actually, the $A(K_s)_{\text{RJCE}}$ overestimation has been previously noticed by Zasowski et al. (2013) and Schultheis et al. (2014a).

The extinction from Gonzalez et al. (2012) does not systematically deviate from our results. The comparison does indicate some outliers, which can be explained by the low resolution map of Gonzalez et al. (2012). There are some stars with large $\log g$ and high T_{eff} , whose extinctions are overestimated by Gonzalez et al. (2012). This confirms Schultheis et al. (2014a)’s finding that the extinction to some of nearby stars have been systematically overestimated in the two-dimensional extinction map.

The extinction difference as functions of distance and extinction itself is presented in Fig.8. The top left panel shows that there is a systematical offset when $d > 9$ kpc. As shown in the left panel of the second row in Fig.7 of Majewski et al. (2011), the RJCE method tends to overestimate extinctions of giants with low $\log g$. Because the fraction of low $\log g$ giants increases with increasing distance in the comparison samples, a systematic offset emerges at greater distance due to RJCE tending to overestimate extinctions for objects with low $\log g$. When comparing our derived extinctions with those from Gonzalez et al. (2012), two sets of data agree very well, with no any noticeable systematic offset for stars with $d > 4$ kpc. However, when $d < 4$ kpc, extinctions from Gonzalez et al. (2012) are consistently lower than ours. Figure 9 of Schultheis et al. (2014a) shows the same trend. The systematic offset may be attributed to the average distance of the tracers that were used to create the extinction map in Gonzalez et al. (2012) being farther away than these relatively close objects. The map overestimated extinctions of these foreground stars.

In the bottom row of Fig.8, we plot the extinction difference versus extinction itself. A systematical offset can be seen in the heavy extinction region, i.e. $A(K_s) > 0.5$, where extinction of RJCE is about ~ 0.1 Mag. lower than ours. A ~ 0.1 difference in the extinction corresponds to about a 5% difference in distance. On the other hand, the extinction from Gonzalez et al. (2012) agrees very well with ours till high extinction, $A(K_s) \sim 0.8$. No systematical offset is seen in the comparison. Above extinction of

$A(K_s) \sim 0.8$, we cannot make any meaningful comparison due to a small sample size.

5.3 Comparison with Three-Dimensional Maps and Models

In this section we compare our derived extinction with the three-dimensional extinction distributions. Several data sets have been used in this comparison.

(i) The 3D extinction map of Chen et al. (2014), which is a three-dimensional extinction map toward Galactic Anticenter area covering Galactic longitude $140^\circ < l < 240^\circ$ deg and latitude $-60^\circ < b < 60^\circ$ deg. By combining photometric data from optical to the near-infrared, they have built a multiband photometric stellar sample of about 30 million stars, and applied spectral energy distribution (SED) fitting to derive this three-dimensional extinction map with spatial angular resolution between $3'$ and $9'$.

(ii) The map of Schultheis et al. (2014b). By using data from the VISTA Variables in the Via Lactea survey together with the Besançon stellar population synthesis model of the Galaxy (Robin et al. 2003, 2012; Chen et al. 2013), Schultheis et al. (2014b) built a 3D extinction map that covers the Galactic bulge region with $-10^\circ < l < 10^\circ$ and $-10^\circ < b < 5^\circ$, which has a resolution of $6' \times 6'$.

(iii) The Drimmel et al. (2003) model. Based on the dust distribution model of Drimmel & Spergel (2001), Drimmel et al. (2003) built a 3D galactic extinction model. This model is constructed by fitting the far- and near-IR data from the *COBE/DIRBE* instrument, with the pixel size of *COBE* being about $21' \times 21'$.

(iv) The Marshall et al. (2006) model, which is built by combining 2MASS near infrared data with the stellar population synthesis model of Besançon (Robin et al. 2003), covering the region of $|l| \leq 90^\circ$ and $|b| \leq 10^\circ$. This map has a spatial resolution of $15'$.

Fig.9 shows the results comparing our Bayesian extinction, $A(K_s)_{\text{Bay}}$ with those derived from two 3D extinction maps, i.e. Chen et al. (2014) and Schultheis et al. (2014b), in which the differences of extinction are plotted against with distance and extinction values, respectively. We cross-match APOGEE stars with the Chen et al. (2014) data set by searching the radius within $3''$. To match with Schultheis et al. (2014b) map, we determine the ex-

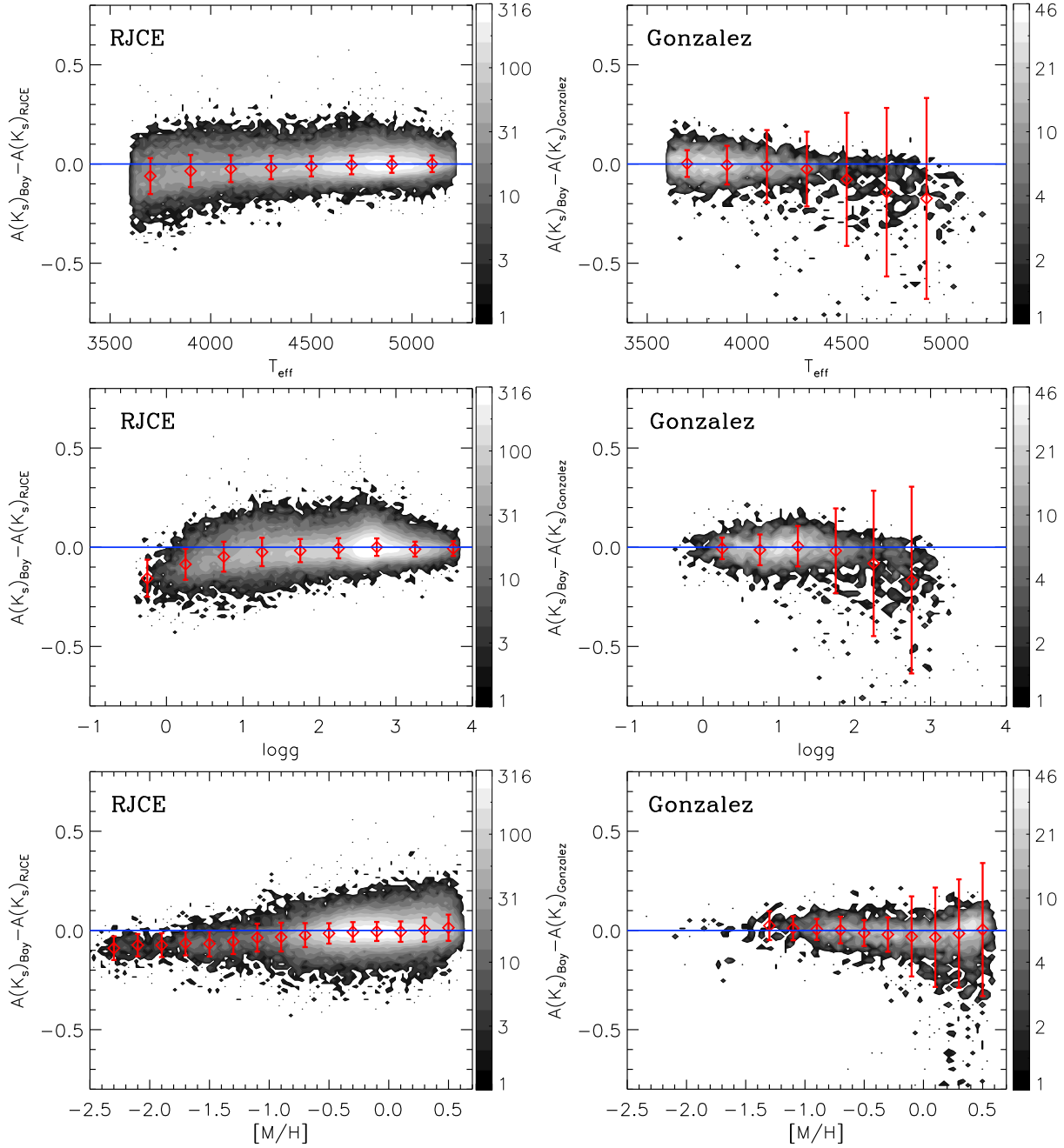


Figure 7. Comparisons of our derived extinction, $A(K_s)_{\text{Bay}}$, to those from RJCE, $A(K_s)_{\text{RJCE}}$ (left column), and G12 $A(K_s)_{\text{Gonzalez}}$ (right column) as a function of T_{eff} , $\log g$, and $[M/H]$. The blue solid lines show the zero. The red symbols show the median values, and the error bar indicates the standard deviation for every bin. The extinction difference shows clear trends with T_{eff} , $\log g$, and $[M/H]$ in the comparison with RJCE, while there is no systematic offset in the comparison with G12 $A(K_s)_{\text{Gonzalez}}$, see text for details

tion of stars by binning the APOGEE stars to a $6'$ resolution, and determine their extinction with the linear interpolation of (distance, $A(K_s)$) from the 3D extinction map. For consistency, all the maps have been re-scaled to $A(K_s)$ using the Cardelli et al. (1989) extinction law. The map of Chen et al. (2014) is built toward the anti-galactic central region, while the Schultheis et al. (2014b) map is toward the bulge region. Our Bayesian extinction is well correlated with that of Chen et al. (2014), such that the mean difference and dispersion are the smallest among these comparisons. There is nearly no systematic offset in the plot of the difference versus

distance (the top left panel of Fig.9), but in the plot of difference against extinction (the bottom left panel of Fig.9) there is a systematic trend that our Bayesian extinction tends to be larger than that in map of Chen et al. (2014) at large extinction.

In the comparison with the 3D extinction map of Schultheis et al. (2014b), there is a systematic trend that our derived extinction is larger than that from Schultheis et al. (2014b) in a nearby region ($d < 7$ kpc), and smaller for $d > 7$ kpc. The reason of the systematic difference in the nearby region is not clear, but it could not come from the saturated magnitude by nearby stars

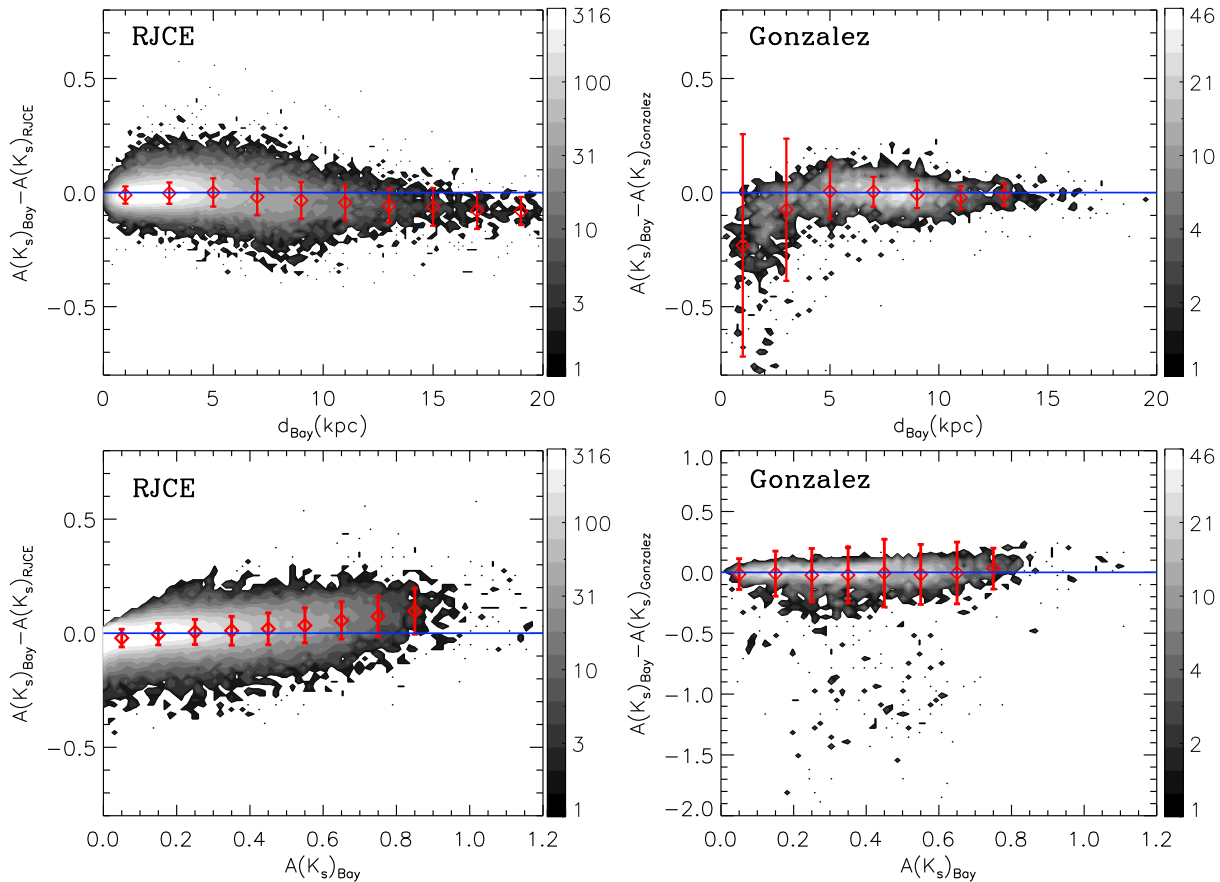


Figure 8. Comparisons of our derived extinction, $A(K_s)_{\text{Bay}}$, with those of RJCE $A(K_s)_{\text{RJCE}}$ (left column), and G12, $A(K_s)_{\text{Gonzalez}}$ (right column) as functions of $A(K_s)_{\text{Bay}}$ and our derived distance d_{Bay} . The red symbols indicate the median values, while error bars show the dispersion in bins.

in the data set of VVV photometry, because the VVV data set is combined with 2MASS counterparts for brighter source. The difference in the distant region may come from the sample selection effect of the APOGEE survey, in which stars with heavy extinction are not observed. However, the samples used in Schultheis et al. (2014b) are complete samples, which have no selection effect. The scatter of difference in extinction is larger than that compared with Chen et al. (2014). This may be partly caused by the high extinction errors of the high extinction in the Galactic Bulge, the errors of the distance and the large variations of extinction in the bins of the 3D extinction map. However, in the comparison with data set of Chen et al. (2014), it is a star to star comparison.

Having calculated the distance and extinction to each of the APOGEE stars, we can easily build our 3D extinction map and compare it with the 3D extinction model. Fig.10 compares our results with the three 3D extinction map toward two different fields. The left panel of Fig.10 shows results toward bulge region ($l = 0.5, b = -2.0$), while the right panel of Fig.10 presents results to the anti-galactic central region ($l = 180.0, b = 0.0$). We queried those 3D extinction maps for the extinction at the position (l, b) of each of our APOGEE bulge stars, within a FOV of 0.25 deg^2 . This FOV was chosen to contain a sufficient number of APOGEE stars with accurate stellar parameters at each spatial position. Because the extinction maps have different spatial resolutions, we took the median value around the center position of each 0.25 deg^2 field. For the field of ($l = 0.5, b = -2.0$), we see that the Schultheis et al. (2014b) model is best matched with our result for region $d > 6$

kpc, while for nearby region $d < 6$ kpc the map of Drimmel et al. (2003) better represents the result. The model of Marshall et al. (2006) predicts a rather steep slope for $d < 4$ kpc. In the comparison with anti-galactic central field ($l = 180.0, d = 0.0$), the maps of Chen et al. (2014) and the model of Drimmel et al. (2003) can give consistent results with ours for $d < 1$ kpc, while for the distant field at $d > 1$ kpc, both maps give lower extinction values comparing to our results.

6 SUMMARY

The APOGEE survey has generated high resolution near-infrared spectra for over 10^5 stars. These data provide valuable information on the studies for Galactic Archaeology. In order to fully exploit these data sets in six-dimension, we used a Bayesian method to derive the distances and extinctions of individual stars by considering photometric and spectroscopic information, as well as prior knowledge on the Milky Way.

All derived distances and extinctions will be made available as online data. Table 3 shows the online data format. The first column is APOGEE ID, the fourth and fifth columns are derived distance and its associated error respectively, while the eighth and ninth columns are estimated extinction and its error respectively. The sixth and seventh columns are another distance indicator, parallax and its error output by the Bayesian method respectively.

To assess the derived distances, we compared our Bayesian

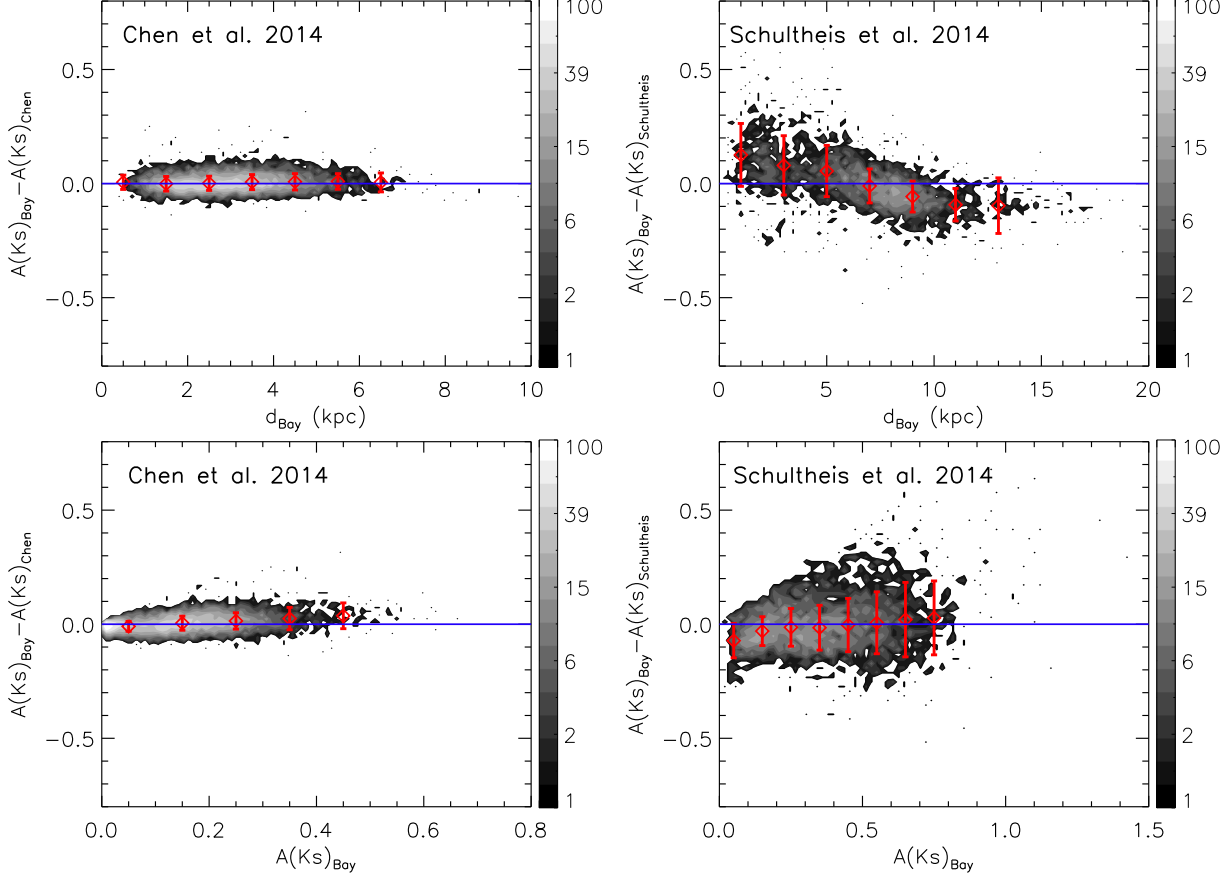


Figure 9. Extinction difference between $A(Ks)$ derived from our Bayesian method, $A(Ks)_{\text{Bay}}$ and that from the 3D extinction map as function of distance and extinction. The 3D extinction maps are from Chen et al. (2014), $A(Ks)_{\text{Chen}}$ and the map of Schultheis et al. (2014b), $A(Ks)_{\text{Schultheis}}$.

Table 3. The derived spectrophotometric distances and extinctions with our Bayesian method for APOGEE stars. The full catalog contains 101726 stars and is only available in electronic form.

apogee_id	R.A. (deg)	Decl. (deg)	$\langle d \rangle$ (kpc)	$\sigma_{\langle d \rangle}$ (kpc)	$\langle \varpi \rangle$ (mas)	$\sigma_{\langle \varpi \rangle}$ (mas)	A_{Ks} (Mag.)	$\sigma_{A_{Ks}}$ (Mag.)
2M12111619+8655554	182.8174591	86.9320755	0.2883	0.0486	3.5608	0.5555	0.0587	0.0201
2M12055981-0307535	181.4992218	-3.1315529	0.1268	0.0149	7.9921	0.9439	0.0058	0.0038
2M12053972+6255594	181.4155121	62.9331703	0.1504	0.0328	6.9261	1.3306	0.0043	0.0027
2M10262280+5424269	156.5950165	54.4074936	0.1289	0.0291	8.1584	1.8269	0.0035	0.0023
2M09451473+2328285	146.3113861	23.4746113	0.1630	0.0267	6.2914	0.9699	0.0065	0.0041

distances to those from four independent measurements, the *Hipparcos* parallaxes, stellar cluster distances, Red Clump star distances, asteroseismic distances from SAGA catalogue (Casagrande et al. 2014) and APOKASC catalogue (Rodrigues et al. 2014). These independent measurements cover four orders of magnitude in distance, from ~ 0.02 kpc (the *Hipparcos* parallaxes) to ~ 20 kpc (star clusters). The results of these validations are all summarized in Table 1. We find that the mean relative difference between our Bayesian distances and those derived from other methods are -4.2% to $+3.6\%$, and that the dispersion ranges from 15% to 25%. Surprisingly, no systematic offset is seen in the comparison with one set of asteroseismic constrained distances (Casagrande et al. 2014). Considering mutual uncertainties in our derived distances and in other measurements, we conclude that, statistically, our derived distances are accurate

to a few percent although errors for a few individual stars could be large. Therefore, they are suitable for statistical studies on Galactic Archaeology.

We have compared our Bayesian extinctions with those derived from the RJCE method. It seems that the extinctions from the RJCE method depend on spectral type. For stars with $T_{\text{eff}} < 4000$ K, $\log g < 1.0$, and $[M/H] < -1.0$, the RJCE method tends to overestimate extinction, however, in most cases this overestimation is less than 0.11 Mag. in K_s -band, which is still within the error budget suggested by Majewski et al. (2011). The overestimation of the extinction at large distance can also be attributed to this effect, as giants with even lower $\log g$ are usually the dominant population at this region due to a selection effect. We also notice that there is a systematic difference at heavy extinction $A(K_s) > 0.8$ Mag., which could be due to the adopted extinction law. Comparing with

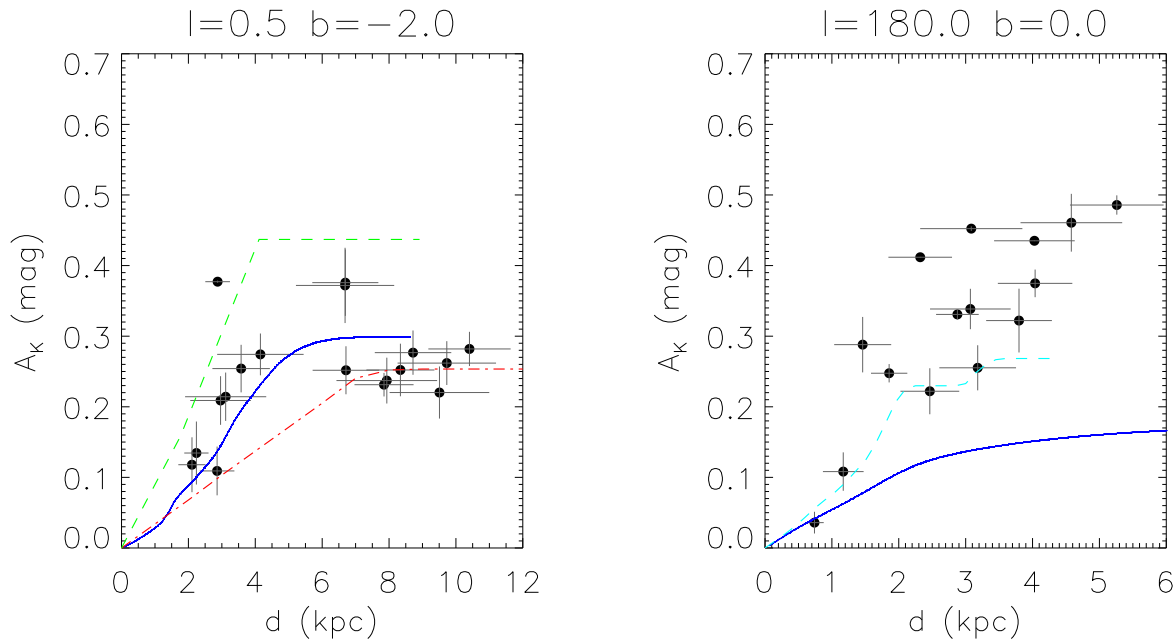


Figure 10. Comparison of 3D extinction map with models in the literature for two fields, one is toward the Galactic bulge region with $l = 0.5$ and $b = -2.0$, and the other one toward the anti-galactic center region with $l = 180.0$ and $b = 0.0$. Dots with error bars indicate result of this work. Left panel: blue line is from Drimmel et al. (2003), red dot-dashed line: Schultheis et al. (2014b), green dashed line: Marshall et al. (2006) Right panel: blue line is from Drimmel et al. (2003), cyan dashed line: Chen et al. (2014).

two dimensional extinction map of Gonzalez et al. (2012), we note that the map may overestimate extinction in the nearby regions.

We also compared our results with three-dimensional extinction models of Drimmel et al. (2003) and maps of Marshall et al. (2006), Schultheis et al. (2014b), and Chen et al. (2014). Compared with our extinction, both the model of Drimmel et al. (2003) and map of Chen et al. (2014) show lower extinction values for distant stars toward the anti-galactic central region. The model of Drimmel et al. (2003) matches well with our results of nearby region ($d < 7$ kpc) toward the bulge field ($l = 0.5, b = -2.0$). For this field the map of Marshall et al. (2006) predicts a steep rise in slope for $d < 4$ kpc, while the map of Schultheis et al. (2014b) provides a good fit with our result for distant region ($d > 7$ kpc).

The accurate distance and extinction derived in the current work provide valuable information for the APOGEE stars, and are important for exploiting the data set of the APOGEE survey when studying the formation and evolution of the Milky Way.

ACKNOWLEDGMENTS

The anonymous referee is greatly thanked for useful comments and suggestions that helped improve the quality of this paper. We warmly thank Diane Feuillet for sharing her *Hipparcos* target list before publishing it and Jon Holtzman for the useful discussion. Haibo Yuan is thanked for useful discussion. This research was supported by the National Key Basic Research Program of China 2014CB845700, and by the National Natural Science Foundation of China under grant Nos. 11321064, 11390371, 11473033, 11428308 and U1331122.

This publication makes use of data products from the Two Micron All Sky Survey, which is a joint project of the University of Massachusetts and the Infrared Processing and Analysis

Center/California Institute of Technology, funded by the National Aeronautics and Space Administration and the National Science Foundation.

This publication makes use of data products from the Wide-field Infrared Survey Explorer, which is a joint project of the University of California, Los Angeles, and the Jet Propulsion Laboratory/California Institute of Technology, funded the National Aeronautics and Space Administration.

Funding for SDSS-III has been provided by the Alfred P. Sloan Foundation, the Participating Institutions, the National Science Foundation, and the US Department of Energy Office of Science. The SDSS-III web site is <http://www.sdss3.org/>.

SDSS-III is managed by the Astrophysical Research Consortium for the Participating Institutions of the SDSS-III Collaboration including the University of Arizona, the Brazilian Participation Group, Brookhaven National Laboratory, Carnegie Mellon University, University of Florida, the French Participation Group, the German Participation Group, Harvard University, the Instituto de Astrofísica de Canarias, the Michigan State/Notre Dame/JINA Participation Group, Johns Hopkins University, Lawrence Berkeley National Laboratory, Max Planck Institute for Astrophysics, Max Planck Institute for Extraterrestrial Physics, New Mexico State University, New York University, Ohio State University, Pennsylvania State University, University of Portsmouth, Princeton University, the Spanish Participation Group, University of Tokyo, University of Utah, Vanderbilt University, University of Virginia, University of Washington, and Yale University.

REFERENCES

Alam, S., Albareti, F. D., Allende Prieto, C., et al. 2015, ApJS, 219, 12

- Ahn C. P. et al., 2014, *ApJS*, 211, 17
- Allende Prieto, C., Majewski, S. R., Schiavon, R., et al. 2008, *Astronomische Nachrichten*, 329, 1018
- An, D., Terndrup, D. M., Pinsonneault, M. H., et al. 2015, *ApJ*, 811, 46
- Bovy, J., Nidever, D. L., Rix, H.-W., et al. 2014, *ApJ*, 790, 127
- Bertelli, G., Bressan, A., Chiosi, C., Fagotto, F., & Nasi, E. 1994, *A&AS*, 106, 275
- Binney, J., Burnett, B., Kordopatis, G., et al. 2014a, *MNRAS*, 437, 351
- Breddels, M. A., Smith, M. C., & Helmi, A., et al. 2010, *A&A*, 511, A90
- Burnett, B., & Binney, J. 2010, *MNRAS*, 407, 339
- Burnett, B., Binney, J., Sharma, S., et al. 2011, *A&A*, 532, A113
- Cardelli, J. A., Clayton, G. C., & Mathis, J. S. 1989, *ApJ*, 345, 245. (CCM)
- Casagrande, L., Silva Aguirre, V., Stello, D., et al. 2014, *ApJ*, 787, 110
- Chen, B. Q., Schultheis, M., Jiang, B. W., et al. 2013, *A&A*, 550, A42
- Chen, B.-Q., Liu, X.-W., Yuan, H.-B., et al. 2014, *MNRAS*, 443, 1192
- Coppola, G., Dall’Ora, M., Ripepe, V. 2011, *MNRAS*, 416, 1056.
- Cui, X.-Q., Zhao, Y.-H., Chu, Y.-Q., et al. 2012, *Research in Astronomy and Astrophysics*, 12, 1197
- Cutri, R. M., Skrutskie, M. F., van Dyk, S., et al. 2003, *The IRSA 2MASS All-Sky Point Source Catalog*, NASA/IPAC Infrared Science
- Cutri, R. M., Wright, E. L., Conrow, T., et al. 2013, *Explanatory Supplement to the AllWISE Data Release Products*, by R. M. Cutri et al. , 1
- Dalessandro, E., Salaris, M., Ferraro, F. R., et al. 2013, *Proc.MNRAS*, 430, 459
- Dalton, G., Trager, S. C., Abrams, D. C., et al. 2012, *Proc.SPIE*, 8446, 84460P
- da Silva, L., Girardi, L., Pasquini, L., et al. 2006, *A&A*, 458, 609
- de Jong, R. S., Bellido-Tirado, O., Chiappini, C., et al. 2012, *Proc.SPIE*, 8446, 84460T
- Dékány, I. & Kovács, G. 2009, *A&A*, 507, 803A
- De Silva, G. M., Freeman, K. C., Bland-Hawthorn, J., et al. 2015, *MNRAS*, 449, 2604
- Dias, W. S., Alessi, B. S., Moitinho, A., & Lépine, J. R. D. 2002, *A&A*, 389, 871
- Drimmel, R., Cabrera-Lavers, A., & López-Corredoira, M. 2003, *A&A*, 409, 205
- Drimmel, R., & Spergel, D. N. 2001, *ApJ*, 556, 181
- Eisenstein, D. J., Weinberg, D. H., Agol, E., et al. 2011, *AJ*, 142, 72
- Fazio, G. G., Hora, J. L., Allen, L. E., et al. 2004, *ApJS*, 154, 10
- Freeman, K. C. 2012, *Galactic Archaeology: Near-Field Cosmology and the Formation of the Milky Way*, 458, 393
- Feuillet, D. K., Bovy, J., Holtzman, J., et al. 2016, *ApJ*, 817, 40
- García Pérez, et al. 2015, *arXiv:1510.07635*
- Koch, D. G., Borucki, W. J., Basri, G., et al. 2010, *ApJL*, 713, L79
- Marshall, D. J., Robin, A. C., Reylé, C., Schultheis, M., & Picaud, S. 2006, *A&A*, 453, 635
- Ness, M., Freeman, K., & Athanassoula, E. 2012a, *Galactic Archaeology: Near-Field Cosmology and the Formation of the Milky Way*, 458, 195
- Ness, M., Freeman, K., Athanassoula, E., et al. 2012b, *ApJ*, 756, 22
- Nishiyama, S., Nagata, T., Kusakabe, N., et al. 2006, *ApJ*, 638, 839
- Nishiyama, S., Nagata, T., Tamura, M., et al. 2008, *ApJ*, 680, 1174
- Nishiyama, S., Tamura, M., Hatano, H., et al. 2009, *ApJ*, 696, 1407
- Holtzman, J. A., Shetrone, M., Johnson, J. A., et al. 2015, *AJ*, 150, 148
- Harris, W. E. 1996, *AJ*, 112, 1487
- Gonzalez, O. A., Rejkuba, M., Zoccali, M., et al. 2012, *A&A*, 543, A13
- Groenewegen, M. A. T. 2008, *A&A*, 488, 935
- Gilliland, R. L., Brown, T. M., Christensen-Dalsgaard, J., et al. 2010, *PASP*, 122, 131
- Girardi, L., Bressan, A., Bertelli, G., & Chiosi, C. 2000, *A&AS*, 141, 371
- Gunn, J. E., Siegmund, W. A., Mannery, E. J., et al. 2006, *AJ*, 131, 2332
- Lindegren, L. 2010, *IAU Symposium*, 261, 296
- Luo, A.-L., Zhao, Y.-H., Zhao, G., et al. 2015, *Research in Astronomy and Astrophysics*, 15, 1095
- Jacobson, H. R., Pilachowski, C., & Friel, E. D. 2011, *AJ*, 142, 59
- Majewski, S. R., Wilson, J. C., Hearty, F., Schiavon, R. R., & Skrutskie, M. F. 2010, *IAU Symposium*, 265, 480
- Majewski, S. R., Zasowski, G., & Nidever, D. L. 2011, *ApJ*, 739, 25
- Marigo, P., Girardi, L., Bressan, A., et al. 2008, *A&A*, 482, 883
- Marigo, P. & Girardi, L. 2007, *A&A*, 469, 239
- Mészáros, S., Holtzman, J., García Pérez, A. E., et al. 2013, *AJ*, 146, 133
- Nidever, D. L., Holtzman, J. A., & Allende Prieto, C., et al. 2015, *AJ*, 150, 173
- O’connell, J. E., Johnson, C. I., Pilachowski, C. A., & Butks, G. 2011, *PASP*, 123, 1139
- Paczynski, B. & Stanek, K. Z. 1998, *ApJL*, 494, L219
- Perryman, M. A. C., de Boer, K. S., Gilmore, G., et al. 2001, *A&A*, 369, 339
- Pinsonneault, M. H., Elsworth, Y., Epstein, C. et al. 2014, *ApJS*, 215, 19
- Pont, F. & Eyer, L. 2004, *MNRAS*, 351, 487
- Robin, A. C., Reylé, C., Derrière, S., & Picaud, S. 2003, *A&A*, 409, 523
- Robin, A. C., Marshall, D. J., Schultheis, M., & Reylé, C. 2012, *A&A*, 538, A106
- Rodrigues, T. S., Girardi, L., Miglio, A., et al. 2014, *MNRAS*, 445, 2758
- Santiago, B. X., Brauer, D. E., Anders, F., et al. 2016, *A&A*, 585, A42
- Sarajedini, A., Dotter, A., & Kirkpatrick, A. 2009, *ApJ*, 698, 1872
- Schultheis, M., Zasowski, G., Allende Prieto, C., et al. 2014a, *AJ*, 148, 24
- Schultheis, M., Chen, B. Q., Jiang, B. W., et al. 2014b, *A&A*, 566, A120
- Schönrich, R., Binney, J., & Asplund, M. 2012, *MNRAS*, 420, 1281
- Skrutskie, M. F., Cutri, R. M., Stiening, R., et al. 2006, *AJ*, 131, 1163
- Steinmetz, M., Zwitter, T., Siebert, A., et al. 2006, *AJ*, 132, 1645
- Williams, M. E. K., Steinmetz, M., Binney, J., et al. 2013, *MNRAS*, 436, 101
- van Leeuwen, F. 2007, *Astrophysics and Space Science Library*, 350,
- Yanny, B., Newberg, H. J., Johnson, J. A., et al. 2009, *ApJ*, 700,

- 1282
Yuan, H. B., Liu, X. W., & Xiang, M. S. 2013, MNRAS, 430, 2188
Wang, J., Shi, J., Zhao, Y., et al. 2016, MNRAS, 456, 672
Wang, J. X., Ma, J., Wu, Z. Y., et al. 2015, AJ, 150, 61
Werner, M. W., Roellig, T. L., Low, F. J., et al. 2004, ApJS, 154, 1
Wu, Z. Y., Zhou, X., Ma, J., et al. 2009, AJ, 133, 2061
Wu, T., Li, Y., & Hekker, S. 2014, ApJ, 786, 10
Wilson, J. C., Hearty, F., Skrutskie, M. F., et al. 2010, Proc,SPIE, 7735, 77351C
Zasowski, G., Johnson, J. A., Frinchaboy, P. M., et al. 2013, AJ, 146, 81
Zhao, G., Chen, Y.-Q., Shi, J.-R., et al. 2006, ChJAA, 6, 265
Zwitter, T., Matijević, G., Breddels, M. A., et al. 2010, A&A, 522, A54